第21回性能に基づく橋梁等の耐震設計に関する
シンポジウム講演論文集（2018年7月）

AN EXPERIMENTAL STUDY ON BUCKLING STRENGTH OF SBHS700 STEEL PLATES WITH CRUCIFORM JOINTS

Nie Jing[1]・Hikaru Sugimoto[2]・Kiyoshi Ono[3]・Takeshi Miyashita[4]・Seiji Okada[5]

[1]Student Member, Waseda University, Department of Civil and Environmental Engineering
（〒169-8555 3-4-1 Okubo, Shinjuku, Tokyo）
[2]Non-member, Waseda University, Department of Civil and Environmental Engineering
[3]Regular Member, Univ. Prof., Dr.-Eng., Waseda University, Tokyo
[4]Regular Member, Univ. Assoc. Prof., Dr.-Eng., Nagaoka University of Technology, Niigata
[5]Regular Member, Dr.-Eng., IHI Infrastructure Systems Co., Ltd.

1. Introduction

In recent years, the use of SBHS (Higher Yield Strength Steel Plates for Bridges) was introduced for its remarkable performance on bridge structures. Considered as a farily new steel material, it has been used on several bridges in Japan including Tokyo Gate Bridge, and it was standardized in JIS G3140[1)]. SBHS can be made with three yield strength grades, which are 400 MPa, 500 MPa and 700 MPa respectively. Comparing to the conventional steels such as SM490Y, the main adtantages of SBHS are high yield strength, toughness and great workability. Moreover, the heat treatment process is required at a much lower level for SBHS. As a high strength grade steel among the three categories of SBHS, SBHS700 is the most effective for long-span bridges. Especially for members such as beam-to-column connections, the design of the thickness of steel plates can be largely reduced comparing to the conventional steels. Therefore, it is significant to investigate on the compressive buckling strength of SBHS700 for future bridge designs.

This paper presents an experimental study on the buckling strength of SBHS700 through conducting compression tests on two test specimens with different width-to-thickness ratio parameters. Based on the experimental data, the load-displacement relationship, strain behavior, out-of-plane deformation as well as the compatibility with the previous standards are thoroughly examined in this study.

2. Experimental design and methodology

(1) Methodology

a) Experimental process

Uniaxial compression tests were conducted on two test specimens with different width-to-thickness ratio parameters R_R. Strain gages were attached on specific locations along the longitudinal direction of both sides on each steel plate. Horizontal and vertical displacement meters were set up after placing the test specimens. At the compressive test, the load was applied with a rate of 0.005 mm/s. After compression, out-of-plane deformation was measured on all plates. Data from strain gages and displacement meters with respect to the load were recorded every two seconds for further investigation.

b) Calculation methods

The calculation of tensile yield load P_y and the corresponding vertical displacement δ_y is shown by Equation (1). The average yield strength σ_y of SBHS700 obtained from the tensile tests is 767 MPa.

$$P_y = \sigma_y A \tag{1a}$$

$$\delta_y = \frac{PL}{EA} \tag{1b}$$

where A: Cross-sectional area;
L : Length of test specimen;
E: Young's modulus.

Width-thickness ratio parameter R_R is defined by:

$$R_R = \frac{b}{t}\sqrt{\frac{12\sigma_y(1-\nu^2)}{\pi^2 E k_R}} \quad (2)$$

where b: width;
t: thickness;
ν: Poisson's ratio (=0.3);
k_R: buckling coefficient (=0.43).

The ultimate strength curve described in "Specifications for highway bridges" by Japan Road Association (JRA) is shown by Equation (3a)[2), 3)]. Another strength curve proposed by Fukumoto et al. from previous surveying studies is described by Equation (3b)[4)].

$$\begin{aligned}\frac{\sigma_{cr}}{\sigma_y} &= 1.0 \quad (R_R \le 0.707)\\ &= \frac{0.5}{{R_R}^2} \quad (R_R > 0.707)\end{aligned} \quad (3a)$$

$$\begin{aligned}\frac{\sigma_{cr}}{\sigma_y} &= 1.0 \quad (R_R \le 0.707)\\ &= \left(\frac{0.7}{R_R}\right)^{0.64} \quad (R_R > 0.707)\end{aligned} \quad (3b)$$

(2) Test specimens

The test specimens are designed according to **Fig. 1** and **Fig. 2.** The cross-section of the columns are made to be cruciform joints, which have three sides welded and one side free for each plate. The dimensions can be found in **Table-1**. The thickness t was fixed to be 9mm, and the width b and length L are different for each test specimen. L was designed so that global buckling was avoided. The columns can be regarded as simply supported. Both vertical and horizontal displacement meters were set on the test specimens before the tests as shown in **Fig. 1** and **Fig. 2**. No apparent initial imperfection was observed by eyes before compression.

(3) Apparatus

A universal testing machine with a total load capacity of 5000 kN as shown in **Fig. 3** was used to conduct compression tests in the present study.

Table-1 Dimensions of the test specimen

	b (mm)	t (mm)	L (mm)	R_R
B07	67	9	250	0.74
B11	105	9	380	1.15

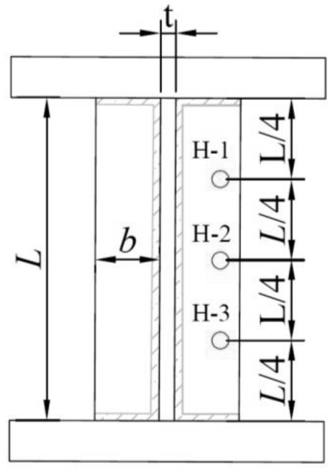

Fig. 1 Design of test specimen (Front view)

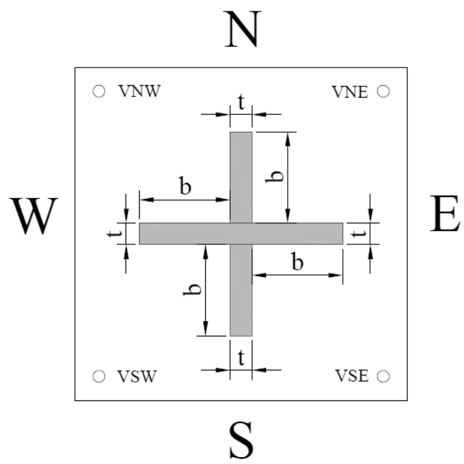

Fig. 2 Design of test specimen (Top view)

Fig. 3 Large-scale testing machine

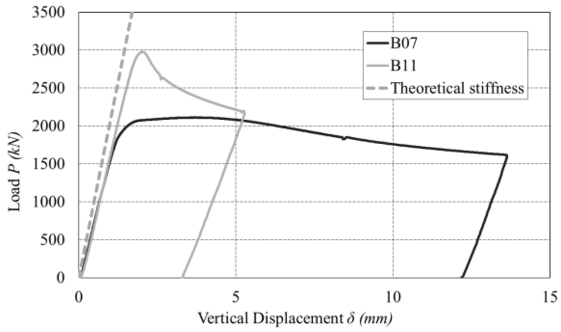

Fig. 4 ***P –δ*** **relationship**

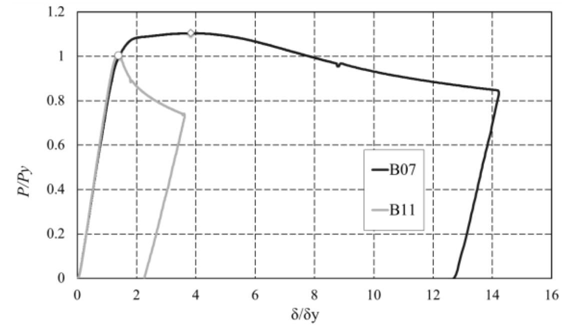

Fig. 5 ***P/P$_y$-δ/δ$_y$*** **relationship**

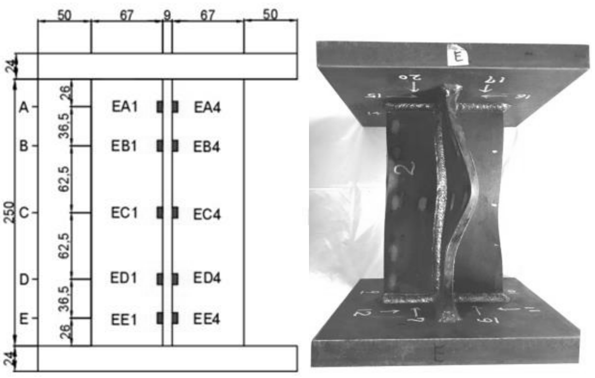

Fig. 6 Strain gages on the East plate of B07

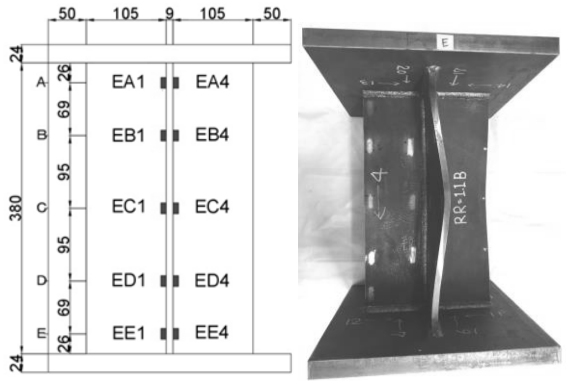

Fig. 7 Strain gages on the East plate of B11

3. Experimental Results

(1) Load- vertical displacement relationship

The *P-δ* relationship can be found in **Fig. 4**. The theoretical line indicating stiffness is shown by the dotted line. The stiffness was calculated based on the Young's modulus *E*, which indicates the theoretical slope at the elastic region of steel. In fact, the calculated theoretical lines of both test specimens were very close, thus only the line of B07 is shown in **Fig.4**. As can be seen, the experimental slopes of B07 and B11 were similar before yielding, yet both lower than the theoretical value. Therefore, the effect of initial imperfection cannot be neglected in the actual experiments.

The results of the normalized *P-δ* relationship can be found in **Fig. 5**, where P_y and δ_y were obtained from the tensile test as calculated in Equation (1). As can be seen, maximum load P_{max} of B11 was very similar to P_y, while B07 reached a higher maximum load at a larger vertical displacement. In addition, differences were also found in the shape of the normalized *P-δ* curve, especially in the behaviors after reaching P_y. For B11, steel plates buckled in the elastic range and a rapid decrease of strength was observed after P_{max}. However, the load of B07 increased to P_{max} with a large vertical displacement after yielding and slowly decreased afterwards in a high range.

(2) Relationship between out-of-plane deformation and buckling phenomenon

a) Strain bifurcation on both sides of steel plate

Strains of East and South plates were measured in this experiment. Strain gages attached at the mid-span of the East plate for both B07 and B11 are shown as examples in **Fig. 6** and **Fig. 7**. Based on the actual deformation of the plates, the mid-spans experience relatively large horizontal displacements among all locations of the strain gages. The load-strain relationships are shown in **Fig. 8** and **Fig. 9**. The strains measured at two sides were highly similar until the bifurcation appeared before reaching the maximum load. The bifurcation of strains was due to out-of-plane deformation casued by plate buckling. Before buckling, little out-of-plane deformation can be observed, while the values of strain on two sides at the same point start to differ with a more distinct out-of-plane deformation. The right-hand side of East plane of both B07 and B11 had transitions

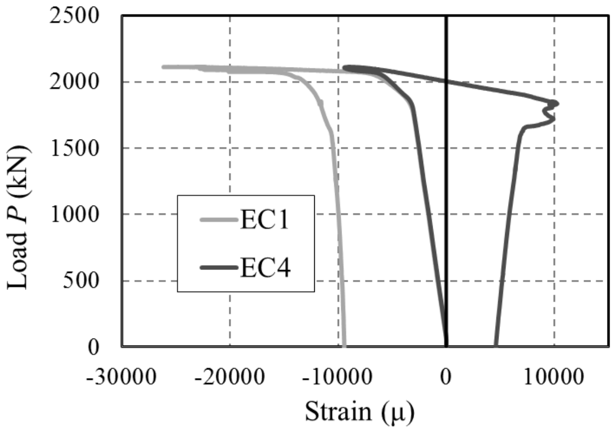

Fig. 8 Strain bifurcation at EC of B07

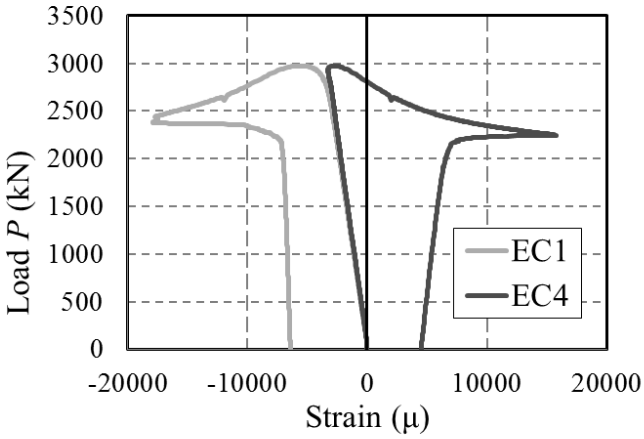

Fig. 9 Strain bifurcation at EC of B11

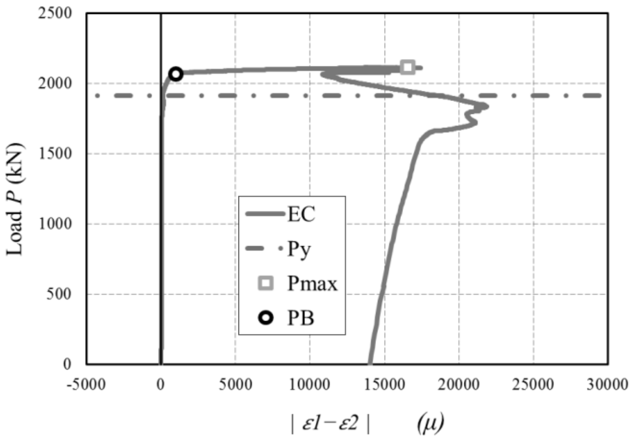

Fig. 10 Strain bifurcation at EC of B07

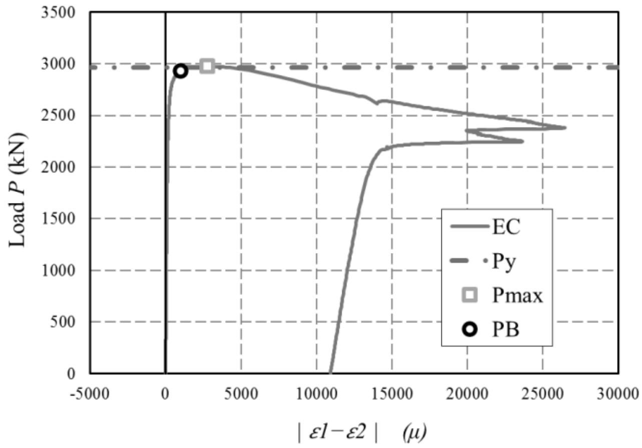

Fig. 11 Strain bifurcation at EC of B11

from compression to tension, which led from a reduction of negative strain to a increase in positive strain as shown in **Fig. 8** and **Fig. 9**.

b) Relationship between strain bifurcation and buckling phenomenon

In order to locate the starting point of buckling, the point when bifurcation occurred was obtained by evaluating the difference of the values of strain on both sides $|\varepsilon_1$-$\varepsilon_2|$. Due to the fact that the same load P was applied on both sides of the plate at the same time, the value of P when $|\varepsilon_1$-$\varepsilon_2|$ suddenly inflected from zero indicates the occurence of large out-of-plane deformation. The relationship between P and $|\varepsilon_1$-$\varepsilon_2|$ on EC of B07 can be found in **Fig. 10**, and that of B11 is shown in **Fig. 11.**

In this study, P_B was determined when $|\varepsilon_1$-$\varepsilon_2|$ is roughly 1000μ, due to the observation of the inflection point in the P -$|\varepsilon_1$-$\varepsilon_2|$ figure. The points of discrepancy of all five locations were obtained in a similar way, and the average value of P_B on the same plate was used as the starting point of buckling. The comparison between P_B, P_{max}, and P_y of B07 and B11 can be found in **Fig. 10** and **Fig. 11**. For B07, P_B was smaller than P_{max} and larger than P_y, which indicated the plate buckled after yielding. As a result, the load decreased gradually after reaching the maximum load due to the effect of both buckling and strain hardening. On the other hand, for B11, P_B was smaller than both P_{max} and P_y. Therefore, the plate buckled within the elastic range, which caused a more sudden decrease of load than B07.

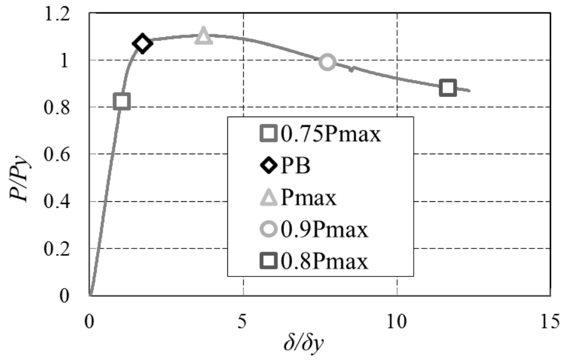

Fig. 12 ***P/P_y-δ/δ_y*** **relationship of B07**

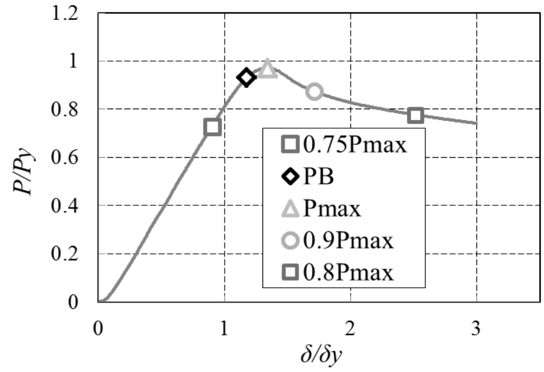

Fig. 13 ***P/P_y-δ/δ_y*** **relationship of B11**

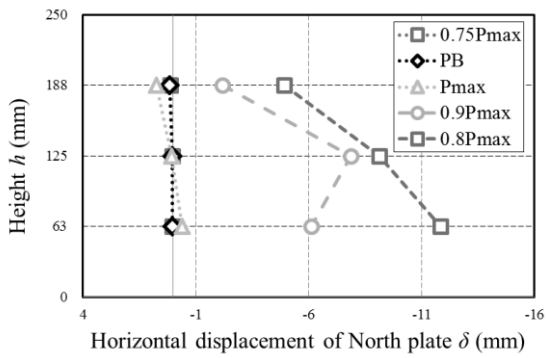

Fig. 14 Out-of-plane deformation of North plate of B07

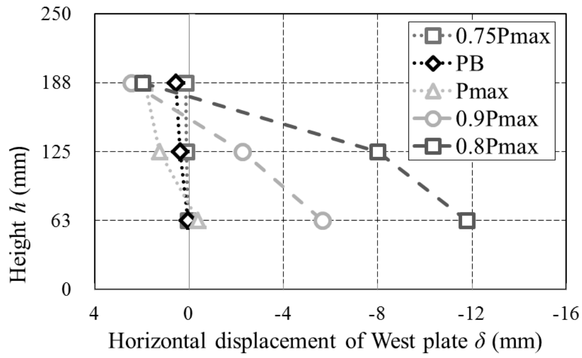

Fig. 15 Out-of-plane deformation of West plate of B07

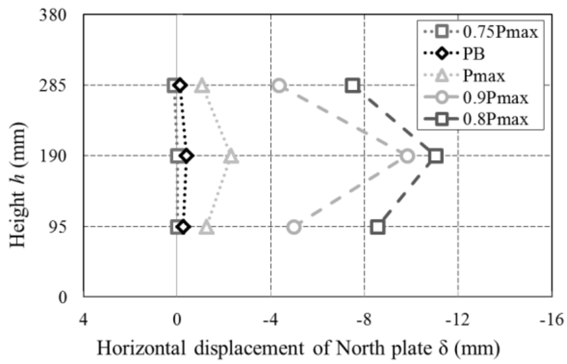

Fig. 16 Out-of-plane deformation of North plate of B11

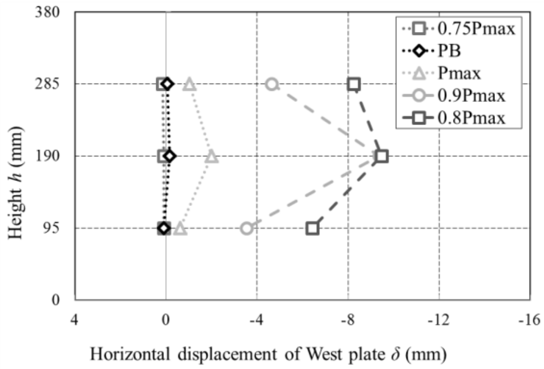

Fig. 17 Out-of-plane deformation of West plate of B11

c) Out-of-plane deformation

The out-of-plane deformation was measured by the horizontal displacement meters attached on the North and West plates. According to the P/P_y-δ/δ_y relationship as shown in **Fig. 12** and **Fig. 13**, five critical points were taken to show the buckling process. Horizontal displacement of B07 can be found in **Fig. 14** and **Fig. 15**, and that of B11 are shown in **Fig. 16** and **Fig. 17**.

As can be observed, little horizontal displacement can be observed before the load reached P_B. However, distinct displacement started to occur after P_{max}. Due to the initial imperfection, plates buckled not at the same time. Therefore it can be concluded that the buckling phenomenon happened after P_B, which corresponded to the results obtained from the strain bifurcation. Moreover, larger vertical displacement can be found on B07 after P_B and before P_{max}. The values of P_B and P_{max} are very similar for both B07 and B11, while B07 experienced larger plastic deformation after buckling.

(3) Comparison with the previous design standards

As an important factor to evaluate the load carrying capacity regarding the safety design margin, the yield ratio σ_{cr}/σ_y was used in the design specifications. It can be calculated as the ratio between the experimental critical stress σ_{cr} based on P_{max}, and the lower yield stress σ_y obtained from the tensile tests. In **Fig. 18**, the two test specimens were plotted on the same graph with the previous design standards described in Equation (3). Both test specimens were above the design methods, which proved its possibility to be evaluated by the previous design standards.

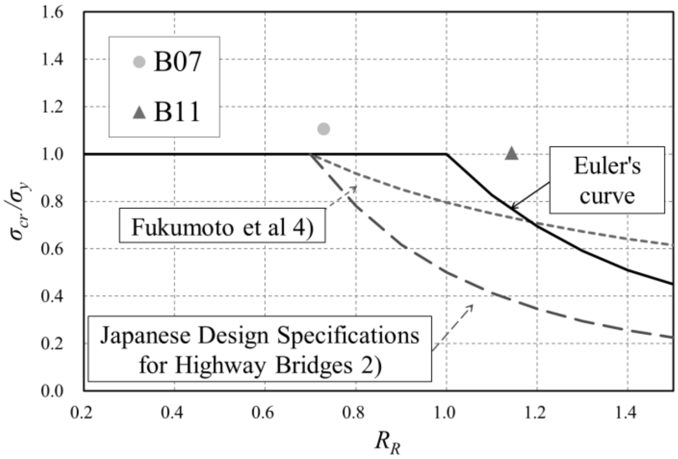

Fig. 18 Comparison with the previous design methods

3. Conclusions

In this study, compression tests were conducted on cruciform columns with two different R_R. With a smaller R_R, the strength increased with a larger vertical displacement after yielding due to strain hardening. However, when R_R is larger, the load carrying capacity of column was mainly controlled by the buckling strength with a more sudden reduction of load right after the maximum load. The starting point of buckling was evaluated by the strain differences on both sides of the plates. The point of buckling obtained corresponded to the occurrence of out-of-plane deformation. Finally, SBHS700 was found to have load carrying capacity that is possible to be evaluated by the previous design specifications. As a matter of fact, the data of the present study are still inadequate to fully evaluate the capacity of SBHS700, thus more experiments and analyses are required in the future studies.

Acknowledgement: This work was supported by the Japan Iron and Steel Federation.

References

1) Japan Industrial Standards Committee: Higher yield strength steel plates for bridges, JIS G3140, 2011. (in Japanese).
2) Japan Road Association (JRA): Specifications for highway bridges, Part II; Steel Bridges, 2012. (in Japanese).
3) Nakai Hiroshi, Hitada Toshiyuki: Bridge engineering [Vol. one], Morikita Publishing Co., Ltd, 1999. (in Japanese)
4) Yushi Fukumoto et al: Approach to The Unified Evaluation of Ultimate Strength of Steel Framed Structures", Achievement Report of Grant-in-Aid for Scientific Research, 1990. (in Japanese)